Available online at www.sciencedirect.com

SCIENCE DIRECT

Developmental Biology 281 (2005) 66 – 77

DEVELOPMENTAL BIOLOGY

www.elsevier.com/locate/ydbio

Cardiac neural crest is necessary for normal addition of the myocardium to the arterial pole from the secondary heart field

Karen L. Waldo, Mary R. Hutson, Harriett A. Stadt, Marzena Zdanowicz, Jaroslaw Zdanowicz, Margaret L. Kirby*

Department of Pediatrics (Neonatology), Neonatal-Perinatal Research Institute, Duke University Medical Center, Bell Building, Room 154, Box 3179, Durham, NC 27710, USA

Received for publication 19 January 2005, revised 19 January 2005, accepted 10 February 2005
Available online 11 March 2005

Abstract

In cardiac neural-crest-ablated embryos, the secondary heart field fails to add myocardial cells to the outflow tract and elongation of the tube is deficient (Yelbuz, T.M., Waldo, K.L., Kumiski, D.H., Stadt, H.A., Wolfe, R.R., Leatherbury, L., Kirby, M.L., 2002. Shortened outflow tract leads to altered cardiac looping after neural crest ablation. Circ. Res. 106, 504–510). Since that study, we have shown that the secondary heart field provides both myocardium and smooth muscle to the arterial pole (Waldo, K.L., Hutson, M.R., Ward, C.C., Zdanowicz, M., Stadt, H.A., Kumiski, D., Abu-Issa, R., Kirby, M.L., 2005. Secondary heart field contributes myocardium and smooth muscle to the arterial pole of the developing heart. Dev. Biol. 281, 78–90). The present study was undertaken to determine whether addition of both cell types is disrupted after neural crest ablation. Marking experiments confirm that the myocardial component fails to be added to the outflow tract after neural crest ablation. The cells destined to go into the outflow myocardium fail to migrate and are left at the junction of the outflow myocardium with the nascent smooth muscle at the base of the arterial pole. In contrast, the vascular smooth muscle component is added to the arterial pole normally after neural crest ablation. When the myocardium is not added to the outflow tract, the point where the outflow joins the pharynx does not move caudally as it normally should, the aortic sac is smaller and fails to elongate resulting in abnormal connections of the outflow tract with the caudal aortic arch arteries.

Keywords: Heart development; Outflow tract; Arterial pole; Myocardium; Smooth muscle; Cardiac neural crest ablation; Secondary heart field

Introduction

Cardiac neural crest cells migrate into pharyngeal arches 3, 4, and 6, and from there, a subpopulation migrates into the cardiac outflow tract to participate in division of the outflow into pulmonary and aortic vascular channels. In addition to this direct role in cardiac development, the crest cells also have an indirect role by modulating pharyngeal FGF signaling (Farrell et al., 2001). In mice, FGF8 signaling appears to be critical for development of structures in the pharynx, as well as the heart. An *Fgf8* hypomorphic allele coupled with a null allele results in phenotypic changes in the developing pharynx and heart that mimic cardiac neural crest ablation in the chick suggesting that FGF8 signaling in the pharynx is important for normal heart development in several species (Abu-Issa et al., 2002; Frank et al., 2002; Hutson and Kirby, 2003).

Another indirect effect of cardiac neural crest ablation is failure of elongation of the outflow tract from the secondary heart field (Yelbuz et al., 2002, 2003). Failure of outflow elongation has also been characterized in the *Fgf8* hypomorphic mouse. It has been known for many years that the outflow tract elongates by addition of cells from an extracardiac population (De la Cruz et al., 1977), but it is only recently that the source of these cells has been described in both chick and mouse (Kelly et al., 2001; Mjaatvedt et al., 2001; Waldo et al., 2001). Waldo et al. (2001) used marking experiments and quail-chick chimeras to show that cells in the pharyngeal mesenchyme caudal to the outflow tract are added to the elongating outflow tract. Using different marking

* Corresponding author. Fax: +1 919 668 1599.
E-mail address: mlkirby@duke.edu (M.L. Kirby).

0012-1606/$ - see front matter © 2005 Elsevier Inc. All rights reserved.
doi:10.1016/j.ydbio.2005.02.011

techniques in chick, Mjaatvedt et al. (2001) reported that the conotruncal myocardium is derived from an anterior heart field which they defined as pharyngeal mesenchyme immediately adjacent and surrounding the distal end of the heart tube. An anterior heart field was identified in mice by Kelly et al. (2001), who used a lacZ transgenic insertion into the mouse Fgf10 locus. In this case, lacZ expression was found in the entire outflow tract and right ventricle (Kelly et al., 2001; Zaffran et al., 2004).

In a previous study, we traced secondary heart field cells by marking them with a combination of DiI and rhodamine at stages 14/15, when elaboration of the distal outflow tract myocardium was initiated, and stages 18/20, when outflow elongation should have ceased (Waldo et al., 2005). Two groups of cells moved from the secondary heart field to the arterial pole. The early group of marked cells added myocardium by moving to the contralateral side of the outflow tract myocardium within 48 h. The second group of cells, marked at later stages were found on the ipsilateral caudal wall of the aortic sac distal to the myocardial edge where vascular smooth muscle markers were expressed. These results showed that the secondary heart field provides both myocardium and vascular smooth muscle to the arterial pole of the heart. Furthermore, the smooth muscle tunic of the aorta and pulmonary trunk was derived from two populations: distally from cardiac neural crest cells and proximally from the secondary heart field. This meant that there were two seams where cells abutted in the arterial pole. The first was at the myocardial junction with secondary heart field-derived vascular smooth muscle and the second was between the secondary heart field-derived vascular smooth muscle and the cardiac neural crest-derived vascular smooth muscle.

In this study, we investigated what effect cardiac neural crest ablation has on the vascular smooth muscle and myocardial populations derived from the secondary heart field. We marked the secondary heart field cells in embryos after neural crest ablation with DiI/rhodamine, and follow their migration over time. We examined the myocardial-to-smooth muscle junction in the arterial pole using vascular smooth muscle, myocardial, and endothelial cell markers in chick and quail embryos. Cardiac neural crest ablation disrupts development of the arterial pole by interfering with addition of the myocardium but not the smooth muscle derived from the secondary heart field. Normally, as the myocardium is added, the outflow tract moves caudally along the ventral pharynx and this movement does not occur after neural crest ablation. As a result, the junction of the outflow tract with the pharynx is abnormal and the formation of the most caudal aortic arch arteries is disrupted. Rather than migrating into the outflow tract and differentiating into myocardium, the progenitor population in the secondary heart field undergoes excessive proliferation in the floor of the pharynx which perturbs the junction of vascular smooth muscle with myocardium. Finally, failure of addition of the myocardial contribution from the secondary heart field results in disrupted patterning of the arterial pole.

Materials and methods

Neural crest ablation

Cardiac neural crest-ablated and sham-operated embryos were prepared as described previously (Waldo et al., 1999). Embryos were collected at stages 12, 14, 16 18, 22, and at day 8.

Secondary heart field cell tracing

Cell tracing was performed as previously described (Waldo et al., 2005).

Cell proliferation

5-Bromo-2′deoxyuridine (BrdU, 20 μl of a 40-mM solution, Boehringer) was applied to the chick embryos 1 h before fixation in 4% paraformaldehyde in PBS as reported by Brand-Saberi et al. (1995). Fixation was carried out overnight followed by paraffin embedding, sectioning, and immunohistochemical processing. The number of BrdU-positive cells was counted in populations of 100 cells in transverse and sagittal sections.

Immunohistochemistry

The embryos were embedded in paraffin, sectioned at 8 μm and processed as described previously (Waldo et al., 1998; Waldo et al., 2005) to visualize HNK1, MF20, QH-1, myosin light chain kinase (MLCK), alpha smooth muscle actin (αSMA), anti-rhodamine and BrdU. The preparations were counterstained with hematoxylin (Anatech, Battle Creek, MI).

In situ hybridization

Cloning, probe preparation, and in situ hybridization for SM22 and Nkx2.5 were described in detail previously (Waldo et al., 2001, 2005). After examination and documentation of whole-mount staining, the embryos were embedded, in 15% sucrose and 7.5% gelatin, frozen and cryo-sectioned at 12 μm and mounted.

Results

Cardiac neural crest ablation disrupts the myocardial but not the smooth muscle contribution to the arterial pole from the secondary heart field

We have recently reported that the secondary heart field first adds myocardium and later smooth muscle to the arterial pole (Waldo et al., 2005). To follow the addition of the secondary heart field cells to the arterial pole in neural crest-ablated embryos more closely, we labeled the secondary heart field of neural crest-ablated

and sham-operated embryos with DiI/rhodamine and observed the movement and differentiation of the labeled cells over the next 72 h. In the sham-operated embryos, migration of the myocardial component at stages 14–18 was followed by movement of the smooth muscle component at stages 22–26 as reported previously (Waldo et al., 2005). When the secondary heart field was labeled in neural crest-ablated embryos at stage 14 (Fig. 1A), the labeled cells never moved beyond the distal rim of the myocardium after 48 h (arrow in Fig. 1B). The secondary heart field cells never added myocardium to the outflow in a spiral as described in normal embryos (Waldo et al., 2005; Ward et al., submitted). The labeled cells were clumped at the junction of the outflow tract with the ventral pharynx (arrow in Fig. 1C) and were not, for the most part, incorporated into the outflow myocardium. This was seen in 5 of 6 neural crest-ablated embryos. When secondary heart field was labeled with DiI/rhodamine in neural crest-ablated embryos at stage 21 (Fig. 1D), the smooth muscle component was added to the caudal wall of the aortic sac (arrow in Figs. 1E–F) and was beginning to express alpha smooth muscle actin (αSMA), a marker of smooth muscle differentiation, but showed no expression of MF20 (Fig. 1G). This was seen in 4 of 4 neural crest-ablated embryos.

These results show that the myocardial cells derived from the secondary heart field are not added to the outflow myocardium after neural crest ablation confirming the report by Yelbuz et al. (2002), and further show that the vascular smooth muscle is added normally.

Outflow tract fails to move caudally after neural crest ablation

Comparison of sagittal sections from sham-operated and cardiac neural crest-ablated embryos at progressively later stages showed that the outflow tract of crest-ablated embryos was not moving caudally with respect to the pharyngeal arches. This was obvious by the relationship of the pharyngeal arch arteries to the position of the outflow tract. Frequently, the arch arteries were malaligned with respect to the lumen of the outflow tract. The degree of malalignment was variable and unpredictable but was most noticeable at stages 24–26 when the outflow tract is normally positioned between pharyngeal arch arteries 4 and 6 in sham-operated embryos (Figs. 2A, B). In neural crest-ablated embryos, the outflow tract was aligned with the 3rd or 4th arch artery (Figs. 2C, D), and the lumen of the 4th arch artery was frequently enlarged (Fig. 2D). Due to this misalignment of the outflow tract with the arch arteries, the flow of blood often took a zig-zag pathway (Figs. 3A–C).

Secondary heart field cells proliferate excessively after neural crest ablation

After neural crest ablation, the secondary heart field fails to add the myocardial component to the arterial pole between stages 14 and 18. We wanted to know if the cells were dying. TUNEL assay showed very little cell death in the secondary heart field in either the sham-operated or

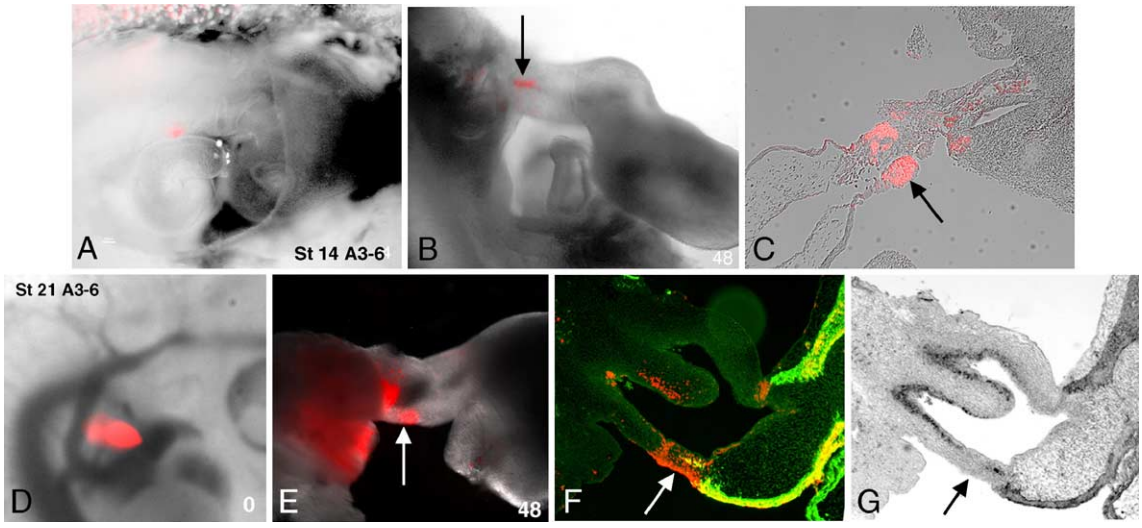

Fig. 1. The myocardial but not the smooth muscle population of the secondary heart field is affected by cardiac neural crest ablation. Cells of the secondary heart field of neural crest-ablated embryos were labeled at stage 14 (A–C) and stage 21 (D–G) with a mixture of DiI and rhodamine (red). (A) 4 h following injection at stage 14; labeled cells located caudal to outflow tract. (B) 48 h following injection; labeled cells distal to outflow tract myocardium (arrow). (C) Sagittal section of the cardiac outflow and aortic sac region (in B) immunostained with rhodamine antibody to identify DiI/rhodamine-labeled cells which are distal to the myocardial rim (arrow). (D) At the time of the injection, labeled cells were caudal to the distal outflow tract. (E) 48 h after injection, labeled cells are in the smooth muscle of the caudal wall of the aortic sac (arrow). (F) Sagittal section from the embryo in E immunostained with rhodamine antibody (red) to identify labeled DiI/rhodamine-labeled cells (arrow) and MF20 (green) to identify myocardial cells. (G) The section in F was relabeled with αSMA (dark gray cells in aortic sac). The majority of the labeled secondary heart field cells are clearly located in the caudal wall of the aortic sac where αSMA is beginning to be expressed (arrow).

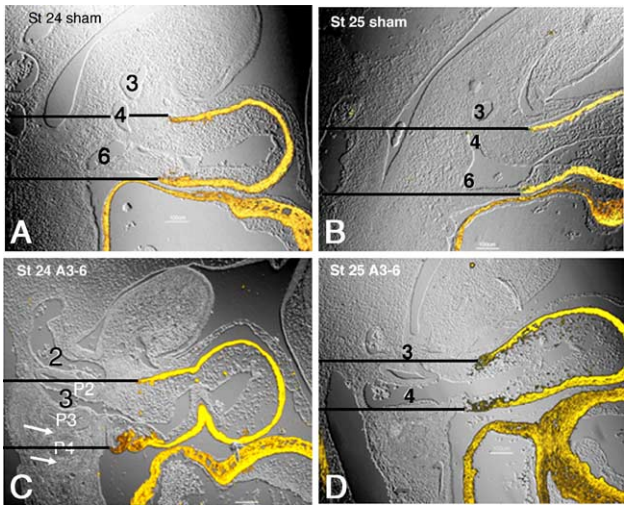

Fig. 2. Cardiac neural crest-ablation disrupts the caudal movement of the outflow tract relative to the pharyngeal arches and its alignment with the aortic arch arteries. MF20 fluorescent images of labeled myocardium (yellow) have been superimposed on sagittal DIC images of the distal outflow tract and pharyngeal arches. The pharyngeal arch arteries are indicated by numbers and the pouches by P accompanied by a number. (A) Normal alignment of the outflow tract lumen at stage 24 compared with alignment in cardiac neural crest-ablated embryo (C) in which the lumen is aligned with the third arch artery. The second arch artery (2) is still open at a time when it should no longer be present, and the 4th and 6th arch arteries are absent (white arrows). By stage 25, the lumen of the outflow tract of a sham embryo (B) is aligned with the 4th and 6th arch arteries. In contrast, the lumen of a neural crest-ablated outflow tract (D) is aligned with an abnormally large 4th arch artery.

neural crest-ablated embryos between stages 14 and 18 (data not shown). BrdU incorporation in sham-operated (n = 40) and neural crest-ablated (n = 41) embryos was used to assess proliferation in the secondary heart field during stages 12–22. Proliferation was significantly increased in the secondary heart field of cardiac neural crest-ablated embryos between stages 14 and 18 (Figs. 4A–E), coinciding with the time during which the myocardial component of the secondary heart field is normally added. At stage 16, proliferation in the outflow myocardium of the neural crest-ablated embryos was elevated to a similar extent while the ventricular myocardium showed slightly less elevated proliferation. By stage 18, proliferation in the secondary heart field of neural crest ablated embryos reached a peak of 300% over control, while proliferation in outflow and ventricular myocardium were decreasing to more normal values (Table 1). At stage 22, when cardiac looping and elongation were complete, there was another increase in proliferation of the secondary heart field in both the sham-operated and cardiac neural crest-ablated embryos (Figs. 4A, F, G). The increased proliferation was associated with re-initiation of HNK-1 expression in the secondary heart field. HNK-1 is associated with cell migration and its re-expression suggests a second wave of movement by the secondary heart field cells that is not disrupted by neural crest-ablation (arrow in Figs. 5A, B). Based on our results from the tracing experiments and from the proliferation data discussed above, the HNK-1 re-expression in the secondary heart field is associated with the generation of vascular smooth muscle cells from the secondary heart field. Because both sham-operated and neural crest-ablated embryos showed the increased proliferation and re-expression of HNK-1, it is likely that the smooth muscle component added by the secondary heart field is normal after neural crest ablation. This further suggests that only the myocardial addition from the secondary heart field is disrupted after neural crest ablation.

Abnormal junction of the outflow tract with the pharynx

The secondary heart field cells in neural crest-ablated embryos are proliferating and have the potential to become cardiomyocytes as evidenced by equivalent expression of Nkx2.5 in both sham-operated and cardiac neural crest-ablated embryos (Supplement, Fig. 1). We examined the secondary heart field cells that remain near the aortic sac of experimental embryos for the myocardial marker, MF20. Sham-operated (n = 57) and cardiac neural crest-ablated (n = 64) embryos were collected at alternating stages between HH14-28 and immunostained with MF20 in whole mount and sagittal sections.

The distal border of the outflow myocardium of crest-ablated embryos was flattened and failed to form in the typical saddle-shape seen in the sham-operated embryos (compare Figs. 6A and B and 6C and D). This saddle-shaped

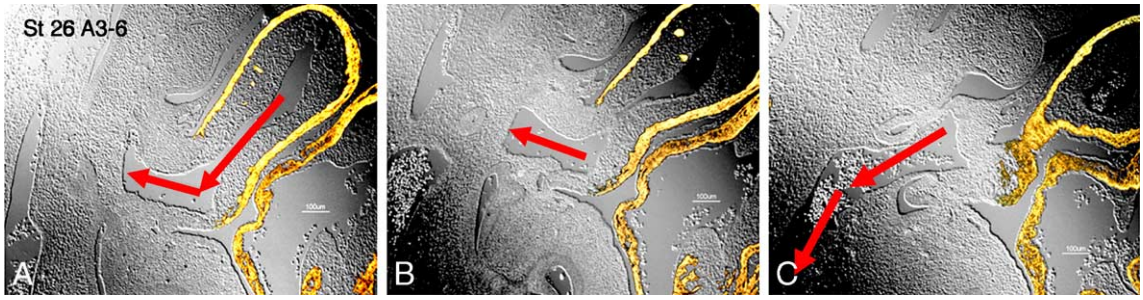

Fig. 3. Abnormal connections of aortic arch arteries with the outflow tract in cardiac neural crest-ablated embryos at stage 26. Fluorescent MF20 images from the same neural crest-ablated embryo were superimposed on DIC sagittal sections. (A–C) The outflow tract has failed to move caudally and is aligned with the fourth arch artery causing the outflow tract lumen to have a zig-zag connection with the lumen of the fourth arch artery.

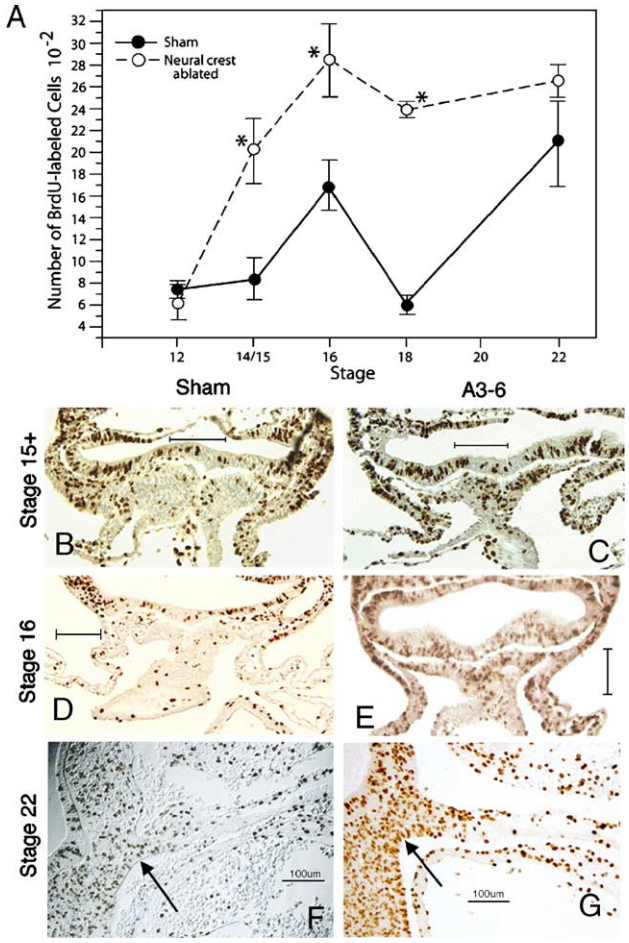

Fig. 4. The secondary heart field experiences two waves of proliferation. (A) The first wave of proliferation occurs during looping and reaches a peak at stage 16 whereas a second wave occurs at stage 22 even though the outflow tract no longer undergoes elongation. After cardiac neural crest-ablation, the secondary heart field cells undergo significantly (*) increased proliferation between stages 14 and 18. Proliferation decreased at stage 18 in the sham-operated but not in neural crest-ablated embryos. At stage 22, the elevation in proliferation in cardiac neural crest-ablated embryos was not significantly compared to shams. (B–E) Transverse sections stained with antiBrdU at stage 15^{+} and 16. Proliferation was elevated in the secondary heart field of the neural crest-ablated embryos (C, E) compared to the shams (B, D). (F, G) Stage 22 sagittal sections stained with antiBrdU. Proliferation was elevated in secondary heart field of both the sham and cardiac neural crest-ablated embryos. Arrow points to the secondary heart field.

border marks the transition from cardiac outflow myocardium to the vascular smooth muscle at the base of the nascent aorta and pulmonary trunk. Furthermore, the distal edge of the myocardial cuff (Figs. 6A–D) was closer to the pharynx in the cardiac neural crest-ablated embryos compared to the shams (compare Figs. 6C and D). This resulted in shortening, or failure of elongation, of the aortic sac region in the cardiac neural crest-ablated embryos (double-headed arrows in Figs. 6C and D). In approximately 40% (14/35 between stages 22 and 26) of the neural crest-ablated embryos, the caudal part of the distal outflow tract and adjoining aortic sac was deformed on one or both sides by bulges that were first recognized at stage 20 and became most prominent at stages 22–24

Table 1
Increased proliferation in secondary heart field and outflow and ventricular myocardium after neural crest ablation

Stage	SHF	Average of inner and outer curvature	
		OFT	Ventricle
16 sham	17	13.5	21
16 NCA	29 (↑ 71%)	23 (↑ 70%)	32 (↑ 52%)
18 sham	6	19.5	27.5
18 NCA	24 (↑ 300%)	25.5 (↑ 31%)	31.5 (↑ 14%)

Number indicates the average number of cells per 100 counted that incorporated BrdU during a 60-min incubation. At least 500 cells were counted for each region.

(asterisks or arrows in Figs. 7A–B′). These bulges were never observed in sham-operated embryos. The walls of these bulges were 30–80% positive for MF20 (white arrows in Figs. 7C, D). Each bulge was partially filled with cardiac jelly and displaced MF20-positive cells. A smaller percentage of embryos had a series of small interconnecting bulges that gave the caudal outflow tract and adjoining aortic sac area a rippled appearance (Fig. 7E, see also Fig. 2C). The bulges extended into the secondary heart field and were directed inward toward the lumen of the aortic sac, or dorsolaterally toward a pharyngeal pouch (green arrows in Figs. 7C–E). In some of these cases, an arch artery (usually the 4th or 6th) was pinched off from the aortic sac by a constriction caused by secondary heart field cells directed toward a 3rd or 4th pharyngeal pouch (Fig. 7E).

In crest-ablated embryos without bulges, the caudal distal edge of the myocardial rim was deformed or thickened by inwardly displaced finger-like extensions of MF20-positive cells (arrows in Fig. 7G) usually directed toward the outflow tract lumen. These deformations differed dramatically from the normal myocardial rim (arrow in Fig. 7F) seen in sham-operated embryos (compare Figs. 7F and G). Sometimes MF20-positive cells were displaced into the subendothelial layer of the caudal aortic sac that eventually becomes the base of the aorta (arrows in Fig. 7H). In addition, because the distal edge of the myocardium failed to regress in cardiac neural

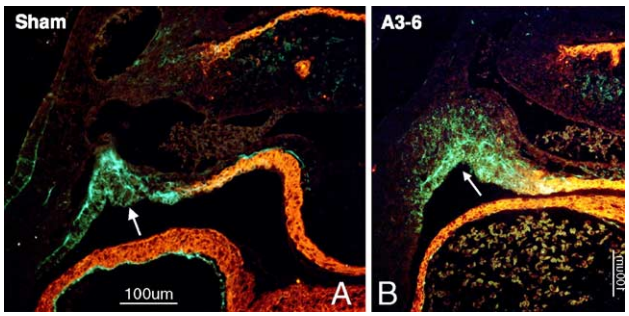

Fig. 5. Reexpression of HNK-1 at stage 22 coincides with generation of secondary heart field-derived vascular smooth muscle. Sagittal sections of the arterial pole were stained with MF20 (red) to identify the myocardium and HNK-1 to identify migrating cells (green). (A, B) Re-expression of HNK-1 at stage 22 in the secondary heart field (arrows) of sham and cardiac neural crest-ablated embryos.

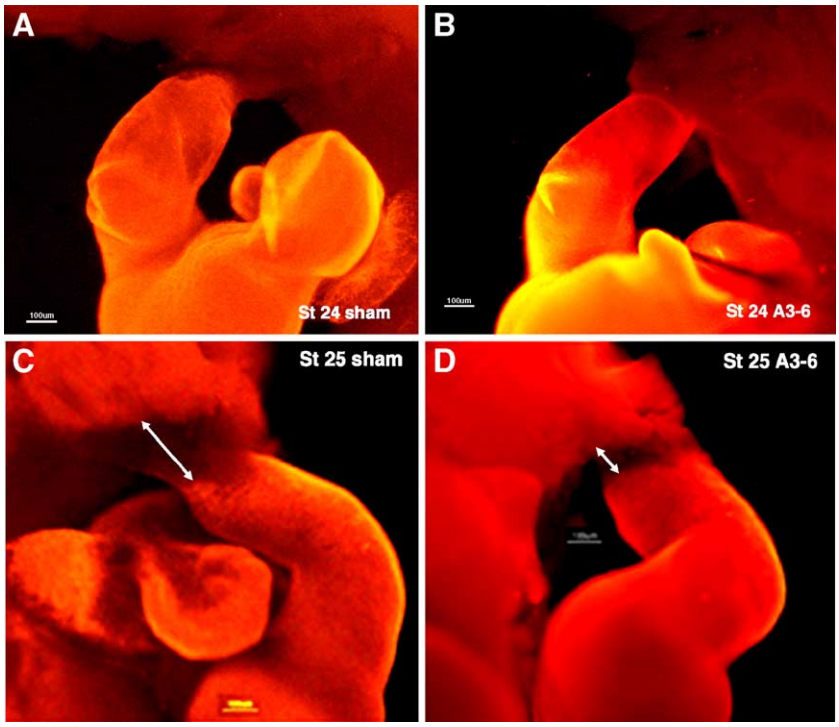

Fig. 6. Abnormal myocardial-smooth muscle junction following cardiac neural crest ablation. Whole mount embryos stained with MF20, a myocardial marker. (A, C) Sham-operated embryos. (B, D) Cardiac neural crest-ablated embryos. At stages 24 and 25, the distal myocardial edge of the outflow tract is flattened in cardiac neural crest-ablated embryos (B, D) and does not achieve the typical saddle-shaped configuration normally seen in sham-operated embryos (A, C). Because the myocardial rim (in D) is more cranially located than normal in the cardiac neural crest-ablated embryos, the adjacent aortic sac region is abnormally shortened (double headed arrow in D). In contrast, the distal myocardial edge (in C) of the sham embryo is located more caudally and the aortic sac region is elongated (double-headed arrow in C).

crest-ablated embryos, the caudal wall of the aortic sac, the part that will become the proximal vascular smooth muscle wall of the pulmonary trunk, was abnormally shortened (compare Figs. 7J and K).

Vascular smooth muscle markers are disrupted by cardiac neural crest-ablation during development of the arterial pole

To determine whether differences exist in the smooth muscle component derived from the secondary heart field in neural crest-ablated embryos, we examined 36 sham-operated and 32 neural crest-ablated embryos between stages 20 and 28 for smooth muscle marker expression. SM22, an early marker of vascular smooth muscle differentiation was examined by in situ hybridization in stage 27 whole mount embryos. By stage 27, SM22 expression was high at the ventriculoarterial junction and on the right side of the aortic sac in sham-operated embryos (arrows in Figs. 8A, B, G). After cardiac neural crest ablation, SM22 expression was detected in all the tissue surrounding the aortic sac (arrows in Figs. 8D–H).

In order to examine the expression of other vascular smooth muscle markers in the arterial pole in cardiac neural crest-ablated embryos, we collected chick and quail embryos at alternating stages between HH22 and 28 and stained with antibodies to αSMA or MLCK. At all the developmental stages observed, cardiac neural crest ablation affected the expression patterns of αSMA and MLCK in a number of ways. Although the subendothelial expression of αSMA and MLCK was not strongly affected by neural crest ablation, the expression of these smooth muscle markers in the mesenchymal tissues adjacent to, or surrounding the aortic sac was profoundly affected. Most often, the αSMA expression tended to be ectopic and disorganized (compare αSMA-positive mesenchyme in Figs. 9A and B). As shown previously, αSMA is associated with neural crest cells at stages 22–28 and is not normally expressed by smooth muscle cells derived from the secondary heart field until stages 28–29 (Waldo et al., 2005). At late stage 28, an area in the proximal wall of the aorta and pulmonary trunk that had been αSMA-negative in earlier stages was αSMA-positive in both sham-operated and cardiac neural crest-ablated embryos (compare Figs. 9C with D). This is the region of smooth muscle derived from the secondary heart field (Waldo et al., 2005). In contrast MLCK was expressed in the same regions as in sham-operated embryos (arrow in Figs. 9F and H).

The aortic sac is diminished in size and does not elongate which results in abnormal aortic arch artery development

Because the outflow tract did not move caudally with respect to the aortic arch arteries in cardiac neural crest-ablated embryos, we investigated how the aortic sac was

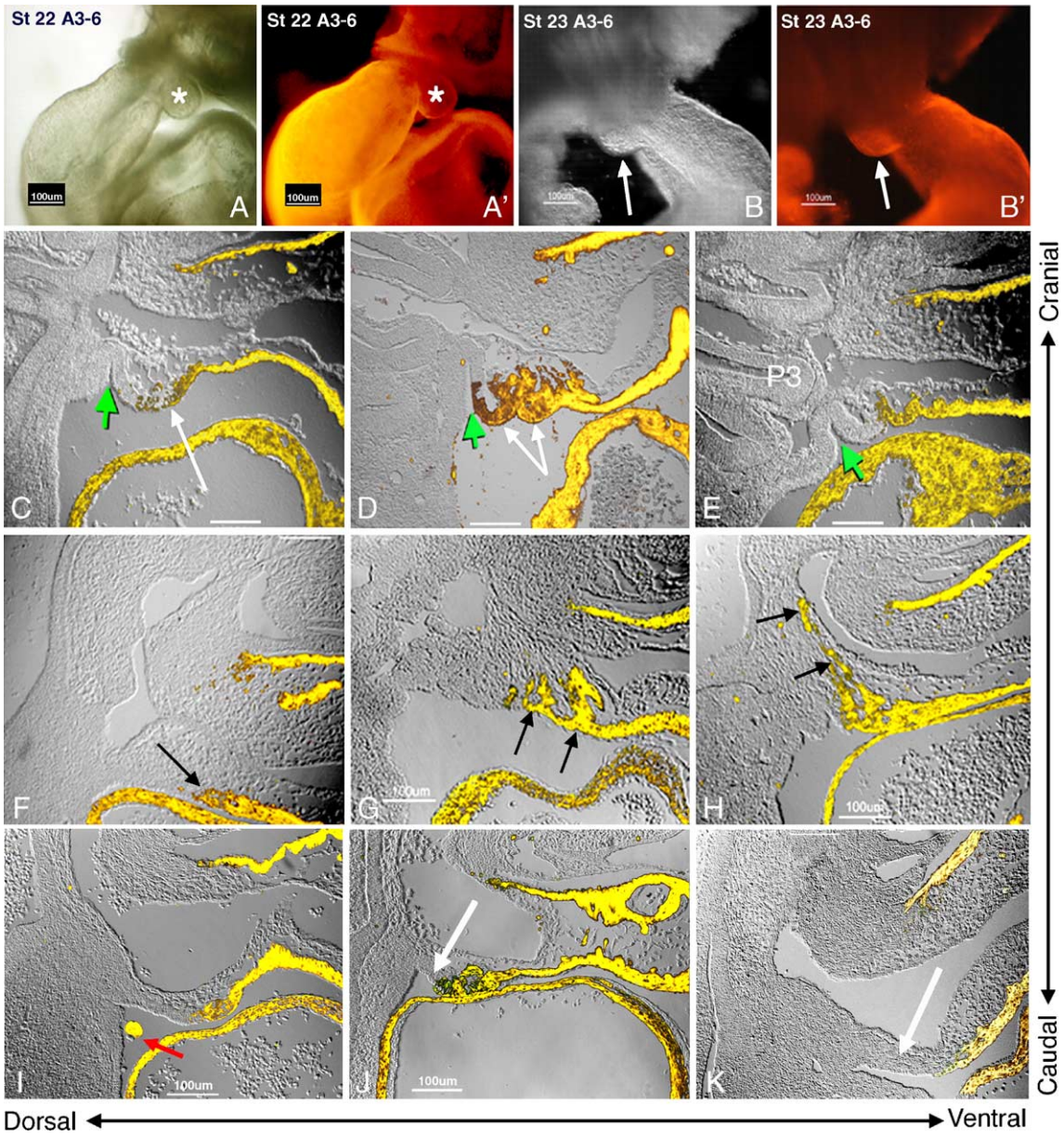

Fig. 7. Cardiac neural crest ablation disrupts the myocardial-smooth muscle junction potentially impeding flow to the caudal arch arteries. The myocardial-smooth muscle junction is disrupted in cardiac neural crest-ablated embryos. (A–B′) Whole mount embryos in bright field (A and B) stained with MF20 (A′ and B′, red) to label the myocardium. (C–K) DIC images of sagittal sections with superimposed fluorescent MF20 staining (yellow). (A–B′) Bulges (asterisks in A and A′, and arrows in B and B′) at the junction of the myocardium with the vascular smooth muscle of the aortic sac. (C) Section through a bulge (white arrow) consisting of distal outflow tract myocardium and aortic sac mesenchyme and bordered dorsally by an indentation of the secondary heart field (green arrow). (D) Section through a double bulge (white arrows) bordered dorsally by an indentation of the secondary heart field (green arrow) that meets the endoderm of third pharyngeal pouch. (E) A series of indentations disrupt the myocardial/vascular smooth muscle junction and form a rippling appearance of the caudal wall of the aortic sac and distal outflow tract myocardium. A major indentation (green arrow) pinches of the 4th and 6th arch arteries from the aortic sac by pushing against the third pharyngeal pouch (P3). (F) The normal appearance of the distal caudal edge of the myocardium (arrow) when stained with MF20. (G) Abnormally displaced MF20-positive cells (arrows) in a cardiac neural crest-ablated embryo (compare with the normal myocardial rim in F). (H) In the midsagittal part of the aortic sac, myocardial cells are displaced abnormally to the roof of the aortic part of the aortic sac (arrows). (I) Clumps of myocardial cells (red arrow) bud into the pericardial cavity. (J, K) The caudal wall of the aortic sac elongates in the sham embryo (K). In contrast, the caudal wall of the aortic sac in the cardiac neural crest ablated-embryo (arrow in J) has not elongated and the myocardial cuff did not retract.

affected. We used QH-1, an antibody that recognizes endothelial cells and endothelial cell precursors (Coffin and Poole, 1988), in sham-operated and cardiac neural crest-ablated quail embryos in order to compare changes in aortic sac shape and size.

Normally, the aortic sac expands caudally as the caudal aortic arch arteries become patent. The aortic sac of the cardiac neural crest-ablated embryos did not expand caudally. The lumen of the aortic sac was diminished in size proximo-distally when compared to the sham-operated embryos (Figs.

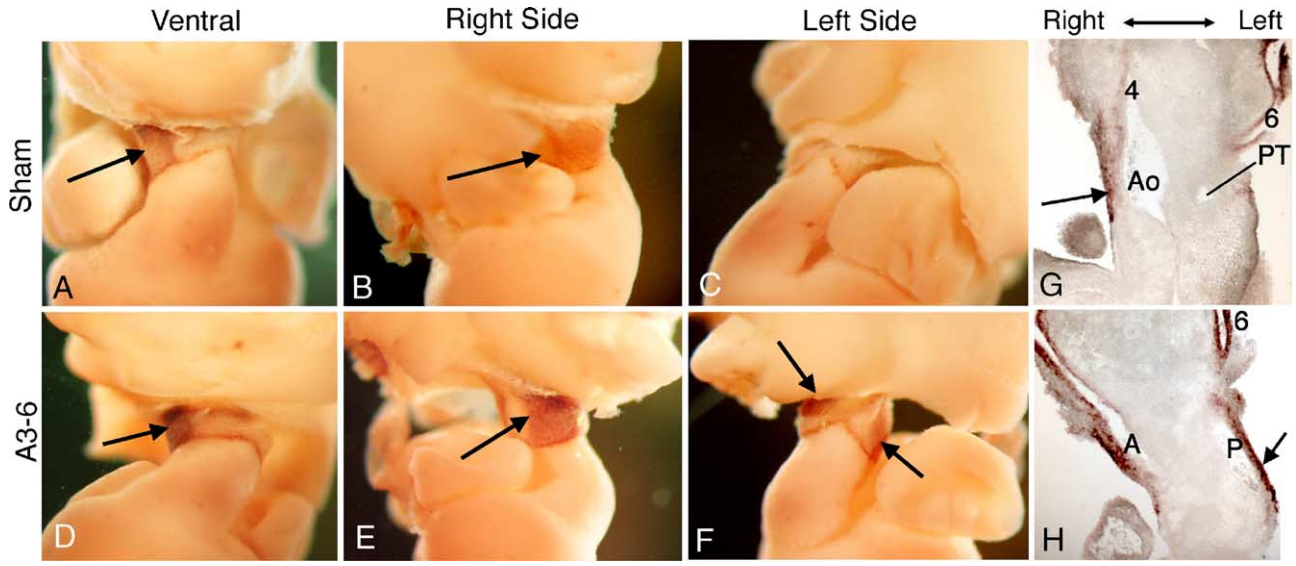

Fig. 8. SM22 is differentially expressed in sham-operated versus neural crest-ablated embryos. Whole mount in situ hybridization at stage 27. (A–C) SM22 expression is higher on the right side in sham-operated embryos when compared to the left side. In contrast, SM22 is high on the left side in cardiac neural crest-ablated embryos and persists in all the tissue surrounding the aortic sac (arrows in D–F). (G, H) Transverse sections of sham (G) and cardiac neural crest-ablated (H) arterial poles showing that SM22 is expressed in all arch arteries (4, 6). In the sham-operated embryo, SM22 expression is higher in the lateral aortic (Ao) wall (arrow in G) and lower in the lateral wall of the pulmonary trunk (PT). In the cardiac neural crest-ablated embryo both the aortic (A) and pulmonary (P) (arrow in H) parts of the aortic sac express SM22 in their outside walls.

10B–D vs. F–H). As a result, the proximal lumens of the arch arteries were diminished in size as they branched from the narrowed aortic sac lumen (compare Figs. 10A with E). The aortic sac in cardiac neural crest-ablated embryos remained close to the pharyngeal floor between stages 22 and 27 instead of becoming translocated ventrally toward the

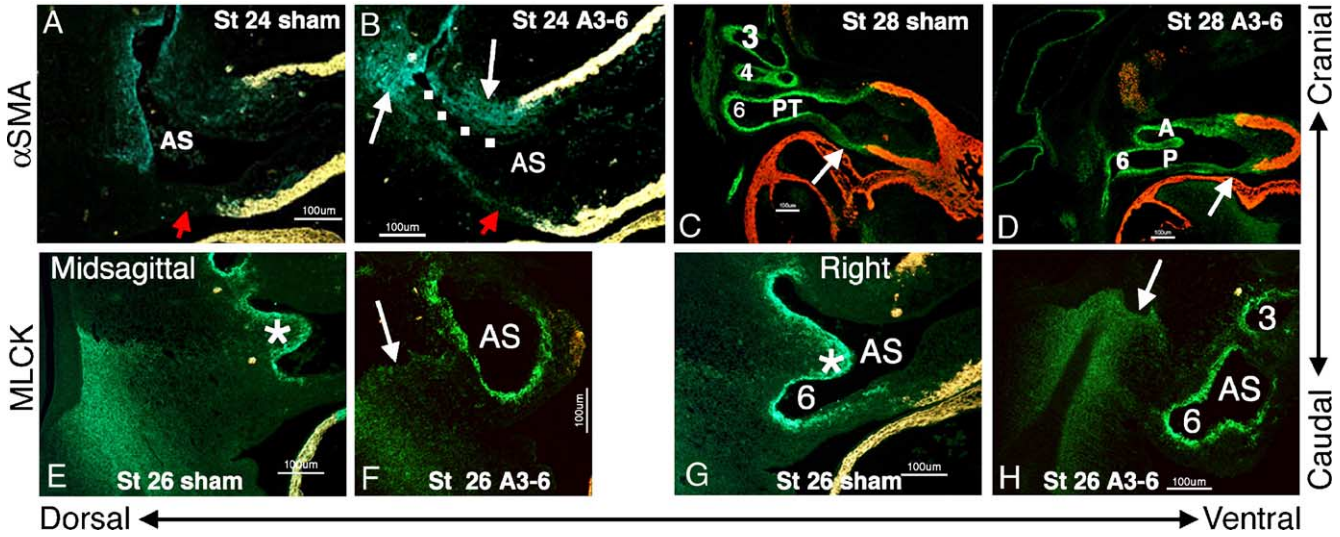

Fig. 9. Cardiac neural crest ablation disrupts the normal expression of vascular smooth muscle markers MLCK and αSMA during development of the arterial pole. (A–D) Sagittal sections of the arterial pole stained with MF20 (red), and αSMA (green or blue green) antibodies. Yellow indicates coexpression of MF20 and αSMA. (E–H) Sagittal sections of the arterial pole stained with MF20 (red) or MLCK (green) antibodies. Yellow indicates coexpression of MF20 and MLCK. At stage 24 (A, B) αSMA is normally expressed subendothelially in the aortic sac (AS) of the sham (A) and neural crest-ablated embryo (B) but in the cardiac neural crest-ablated embryo it is ectopically expressed and disorganized adjacent to the aortic sac (white and red arrows). Dotted line indicates closed lumen of aortic sac. (C, D) At stage 28 the proximal walls of the sham pulmonary trunk (PT) express αSMA (arrows) even though in earlier stages these parts of its walls were αSMA-negative. (E, F and G, H) MLCK expression is compared in stage 26 sham (E, G) and cardiac neural crest-ablated (F, H) embryos (F is a photocomposite of two adjacent images of the same section). MLCK expression is normal in the roof of the aortic sac and the pharyngeal floor but in neural crest-ablated embryos the anterior edge of the MLCK expression (arrow) in the roof of the aortic sac is positioned more cranial than normal. 3, 4, 6 = aortic arch artery number. AS = aortic sac. * = aorticopulmonary septum.

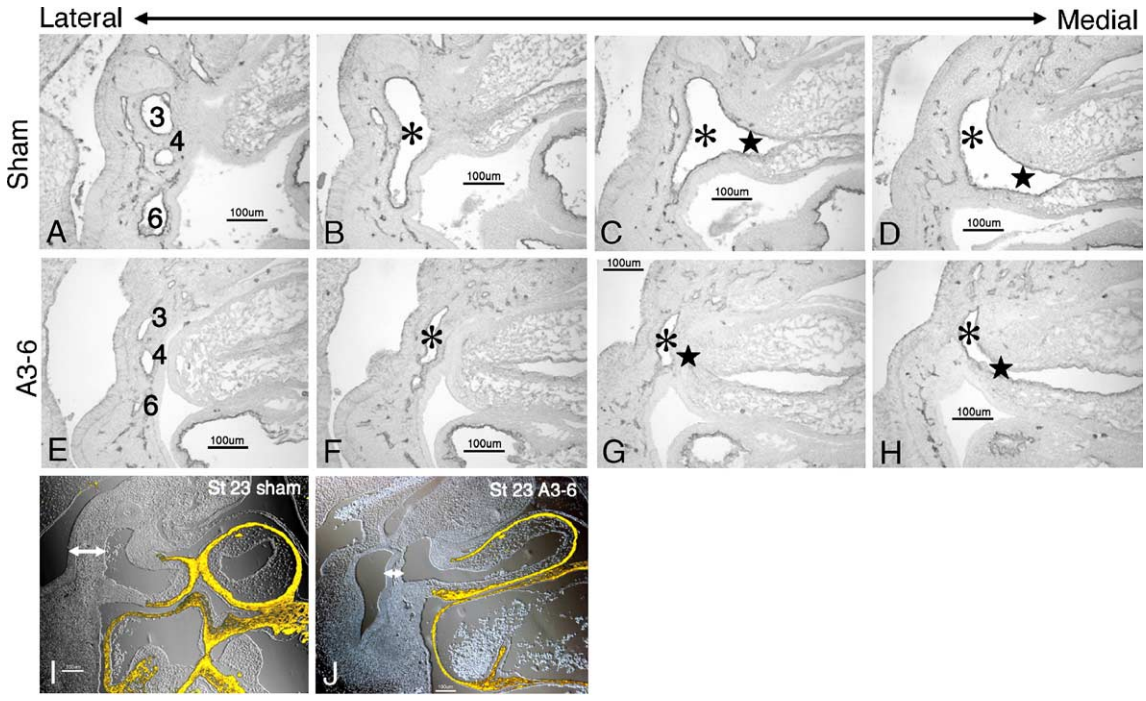

Fig. 10. The size of the aortic sac is diminished and growth towards the heart is delayed in the cardiac neural crest-ablated embryos. (A–H) Sagittal sections of quail aortic sac and the distal outflow tract region stained with QH-1, a marker for quail endothelium and endothelial precursors. (I, J) DIC images of sagittal sections stained with MF20 (yellow). The aortic sac of a sham-operated embryo (A–D) is compared with that of a cardiac neural crest-ablated embryo (E–H). The lumen of the base of the arch arteries (3, 4, 6) as they branch from the aortic sac is greatly diminished in cardiac neural crest-ablated embryos (compare E with A). The lumen of the distal part of the aortic sac (asterisk) of neural crest-ablated embryos is much shorter cranialcaudally and flattened ventrodorsally (compare F with B, G with C, H with D). The lumen of the proximal part of the aortic sac (star in C, D, G, H) is also diminished (compare G with C, H with D). (I, J) In the sham embryo (I), the mesenchyme between the roof of the aortic sac and the foregut endoderm (double-headed arrow) increases in volume, pushing the aortic sac towards the heart. This does not occur in neural crest-ablated embryos (J) and the aortic sac stays close to the foregut floor.

heart (Figs. 10I, J). As a result, the arch arteries were shortened as a consequence of the retained constant distance between the pharyngeal floor and the aortic sac.

Discussion

Based on marking studies in cardiac neural crest-ablated embryos, the myocardial component of the secondary heart field failed to incorporate into the outflow tract and stopped migration at the junction of the outflow tract with the ventral pharynx. Although neural crest ablation blocked production of myocardium by the secondary heart field, it did not affect the production of a vascular smooth muscle tunic for the arterial trunk (Fig. 11). The marking study in cardiac neural crest-ablated embryos is direct confirmation of an earlier observation by Yelbuz et al. (2002) based on altered HNK1 expression that neural crest ablation results in the shortened outflow tract due to the failure of the addition of myocardium from the secondary heart field. Since the Yelbuz et al. study, we have shown that the secondary heart field gives rise to both myocardium and arterial smooth muscle at the arterial pole (Waldo et al., 2005). The present study shows that only the myocardium from the secondary heart field is affected by neural crest ablation. We show that the secondary heart field cells undergo abnormal proliferation rather than initiating migration into the outflow tract and differentiating into myocardium.

Our results further show that cardiac neural crest ablation causes cells in the secondary heart field to lose their ability to migrate as a cohesive group. This is reflected in the morphogenesis of the secondary heart field epithelium. Normally, the secondary heart field is comprised of a pseudostratified epithelium that is distinctive from surrounding tissue. In the neural crest ablated-embryos, the secondary heart field epithelium is disorganized and the secondary heart field cells are displaced inwardly, rather than being maintained in the same tissue plane as the myocardium, as they migrate and incorporate into the myocardium of the distal outflow. Preliminary data in a separate study has shown that the secondary heart field cells normally express Cx43, a protein associated with cell migration in mice (Hutson et al., 2005). We believe that the loss of Cx43 in the neural crest-ablated secondary heart field may explain why the epithelium loses its continuity.

Failure of the myocardial precursors to migrate from the secondary heart field into the outflow tract at the appropriate time resulted in ectopic myocardium that was displaced inwardly toward the lumen of the aortic sac region and the distal outflow tract where it formed bulges in the caudal

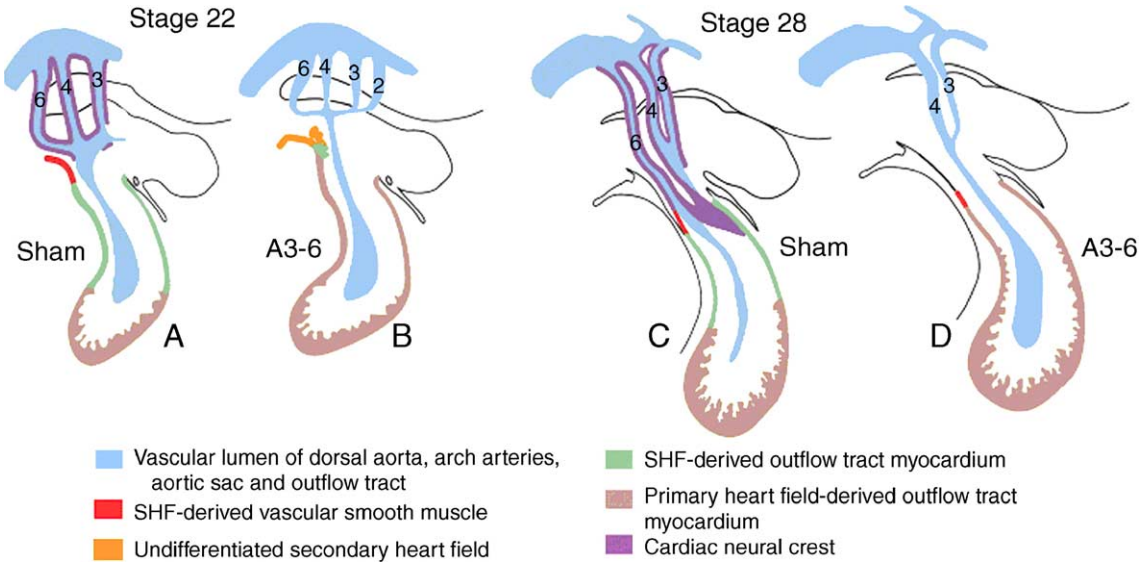

Fig. 11. Diagrammatic representation of the effects of cardiac neural crest ablation on the development of the arterial pole. Panels A and C are reprinted from Waldo et al., (2005). See discussion for details.

myocardial rim and abnormal indentations in the caudal aortic sac mesenchyme. The indentations encroached on the aortic sac and caudal pharyngeal pouches potentially obstructing the blood flow from the aortic sac into the caudalmost arch arteries. This could explain the randomized patterning of the aortic arch arteries after neural crest ablation (Bockman et al., 1987).

Another effect of cardiac neural crest ablation was the failure of the outflow tract to translocate caudally as the caudal aortic arch arteries opened. Because the outflow tract did not move caudally, the distal aortic sac failed to elongate caudally to connect with the caudal most aortic arch arteries. As a result, the 4th and/or 6th arch arteries were often missing, and alignment of the outflow tract with the arch arteries was disturbed. In addition, cardiac neural crest ablation resulted in abnormal proliferation that was most pronounced in the secondary heart field but extended to the myocardium during looping. We believe the increase in proliferation is due to an excess of growth factor signaling in the pharyngeal arches. We have recently shown that FGF8 antibody can rescue many of the effects of cardiac neural crest ablation including increased proliferation and that excessive FGF8 is responsible for increased proliferation by the myocardium (Hutson et al., 2005; Farrell et al., 2001). Interestingly, a recent publication by Xu et al. (2004) shows that *Tbx1* is expressed in mouse secondary heart field where it regulates the cell proliferation, most likely mediated by FGF10, a direct target of Tbx1, and possibly other FGFs. Tbx1 is a T-box transcription factor that is located in the 22q11.2 locus. Deletion of the 22q11.2 locus in humans causes DiGeorge syndrome and is associated with outflow malalignment defects, such as tetralogy of Fallot, and aortic arch artery defects. In the mouse, loss of Tbx1 function causes hypoproliferation in the secondary heart field and hypoplasia of the outflow tract myocardium. This is in contrast to neural crest ablation where we see hyperproliferation of the secondary heart field and shortened outflow tract myocardium.

An additional effect of cardiac neural crest ablation was shortening of the aortic sac caused by the failure of the distal myocardial edge to regress toward the heart. Due to absence of cardiac neural crest cells, the mesenchyme between the roof of the aortic sac and the pharyngeal floor did not expand. As a result, normal translocation of the aortic sac toward the heart and elongation of the aortic arch arteries was delayed until stage 28. Fig. 11 summarizes many of the effects of cardiac neural crest-ablation on the development of the arterial pole.

Normal development of the secondary heart field depends on appropriate levels of FGF signaling. Ablation of cardiac neural crest, which causes a functional increase in FGF signaling (Farrell et al., 2001; Hutson et al., 2005), prevents normal addition of the myocardium from the secondary heart field to the developing cardiac outflow tract. The impact of this failure is that the looped tube is shortened, which prevents convergence of the outflow and inflow limbs, and ultimately results in failure of aortic wedging between the mitral and tricuspid valves. In this case the aorta overrides the ventricular septum and is called dextroposed aorta (Hutson et al., 2005; Yelbuz et al., 2002). This is one component in conotruncal defects such as tetralogy of Fallot and double outlet right ventricle (Tomita et al., 1991). In the neural crest-ablated embryo, the outflow tract is not septated but the degree of wedging of the aortic side of the persisting truncus can be ascertained, and the truncus is most often not in correct alignment (Farrell et al., 1999). Failure of addition of myocardium from the secondary heart field is thus a potential mechanism for genesis of these defects.

Until recently, we did not understand how the neural crest could affect development of the secondary heart field since the two fields of cells are not in direct contact (Waldo et al., 1996). We now know that FGF8 signaling is critical for addition of the secondary heart field to the outflow tract because it can be rescued after neural crest ablation by blocking FGF signaling to bring it to a more normal level (Farrell et al., 2001; Hutson et al., 2005).

Arch artery patterning after neural crest ablation

We have previously documented abnormal persistence and regression of the aortic arch arteries in neural crest-ablated embryos (Bockman et al., 1987; Kirby et al., 1997). The persistence and regression of the arch arteries has been thought to be under the control of genetically encoded patterning instructions (Kirby et al., 1997); however, our current data showing hemodynamically challenged connections between the arch arteries, the aortic sac, and the outflow tract make it possible that normal addition of the secondary heart field and regression of the outflow tract along the ventral pharynx could, in part, impact on arch artery remodeling to the adult configuration. Interestingly, FGF8 expressed by the pharyngeal ectoderm is also important in genesis of the 4th arch artery (Macatee et al., 2003). FGF8 signaling after neural crest ablation is abnormal and so the abnormal patterning of the arch arteries could be due to a variety of factors.

Thus, there are at least four reasons why the aortic arch arteries may be abnormal after neural crest ablation. (1) Absence of neural crest cells around the arch arteries may make them unstable or may mean that patterning instructions are lacking (Kirby et al., 1997). (2) The FGF signaling in the pharynx is excessive after neural crest ablation (Farrell et al., 2001; Hutson et al., 2005). The Fgf8 hypomorphic mouse has abnormal patterning of the aortic arch arteries and great arteries therefore the correct level (not too much and not too little FGF8) may be critical for arch artery patterning (Abu-Issa et al., 2002; Frank et al., 2002; Macatee et al., 2003). (3) Because the outflow tract does not move caudally as it should, the connection of the outflow with the caudal arches is abnormal. (4) Reduction of the size of the aortic sac and/or the abnormal myocardial accumulation at junction of the outflow tract with the myocardium could restrict blood flow or alter hemodynamics at the junction of the outflow with the arch vessels (Clark, 1986). It will be important to consider all of these factors, which are not mutually exclusive, in determining the etiology of arch artery patterning anomalies.

Acknowledgments

We thank Ping Zhang for preparation of the SM22 probe. We are grateful to Radwan Abu-Issa, Erik Meyers and Tony Creazzo for continuing discussions and critical reading of the manuscript. Supported by PHS grants HL36059, HL70140, and HD39946.

Appendix A. Supplementary data

Supplementary data associated with this article can be found, in the online version, at doi:10.1016/j.ydbio.2005.02.011.

References

Abu-Issa, R., Smyth, G., Smoak, I., Yamamura, K., Meyers, E.N., 2002. Fgf8 is required for pharyngeal arch and cardiovascular development in the mouse. Development 129, 4613–4625.

Bockman, D.E., Redmond, M.E., Waldo, K., Davis, H., Kirby, M.L., 1987. Effect of neural crest ablation on development of the heart and arch arteries in the chick. Am. J. Anat. 180, 332–341.

Brand-Saberi, B., Seifert, R., Grim, M., Wilting, J., Kuhlewein, M., Christ, B., 1995. Blood vessel formation in the avian limb bud involves angioblastic and angiotrophic growth. Dev. Dyn. 202, 181–194.

Clark, E.B., 1986. Cardiac embryology: its relevance to congenital heart disease. Am. J. Dis. Child. 140, 41–44.

Coffin, J.D., Poole, T.J., 1988. Embryonic vascular development: immunohistochemical identification of the origin and subsequent morphogenesis of the major vessel primordia in quail embryos. Development 102, 735–748.

De la Cruz, M.V., Gomez, C.S., Arteaga, M.M., Arguello, C., 1977. Experimental study of the development of the truncus and the conus in the chick embryo. J. Anat. 123, 661–686.

Farrell, M.J., Stadt, H., Wallis, K.T., Scambler, P., Hixon, R.L., Wolfe, R., Leatherbury, L., Kirby, M.L., 1999. HIRA, a DiGeorge syndrome candidate gene, is required for cardiac outflow tract septation. Circ. Res. 84, 127–135.

Farrell, M.J., Burch, J.L., Wallis, K., Rowley, L., Kumiski, D., Stadt, H., Godt, R.E., Creazzo, T.L., Kirby, M.L., 2001. FGF-8 in the ventral pharynx alters development of myocardial calcium transients after neural crest ablation. J. Clin. Invest. 107, 1509–1517.

Frank, D., Fotheringham, L., Brewer, J., Muglia, L., Tristani-Firouzi, Capecchi, M., Moon, A., 2002. An Fgf8 mouse mutant phenocopies human 22q11 deletion syndrome. Development 129, 4591–4603.

Hutson, M.R., Kirby, M.L., 2003. Neural crest and cardiovascular development: a 20-year perspective. Birth Defects Res. Part C Embryo Today 69, 2–13.

Hutson, M.R., Stadt, H.A., Burch, J., Creazzo, T.L., Kirby, M.L., 2005. Cardiac outflow alignment is sensitive to levels of FGF8 signaling in the pharynx. (submitted).

Kelly, R.G., Brown, N.A., Buckingham, M.E., 2001. The arterial pole of the mouse heart forms from Fgf10-expressing cells in pharyngeal mesoderm. Dev. Cell 1, 435–440.

Kirby, M.L., Hunt, P., Wallis, K.T., Thorogood, P., 1997. Normal development of the cardiac outflow tract is not dependent on normal patterning of the aortic arch arteries. Dev. Dyn. 208, 34–47.

Macatee, T.L., Hammond, B.P., Benjamin, R., Arenkiel, B.R., Francis, L., Frank, D.U., Moon, A.M., 2003. Ablation of specific expression domains reveals discrete functions of ectoderm- and endoderm-derived FGF8 during cardiovascular and pharyngeal development. Development 130, 6361–6374.

Mjaatvedt, C.H., Nakaoka, T., Moreno-Rodriguez, R., Norris, R.A., Kern, M.J., Eisenberg, C.A., Turner, D., Markwald, R.R., 2001. The outflow tract of the heart is recruited from a novel heart-forming field. Dev. Biol. 238, 97–109.

Tomita, H., Connuck, D.M., Leatherbury, L., Kirby, M.L., 1991. Relation of

early hemodynamic changes to final cardiac phenotype and survival after neural crest ablation in chick embryos. Circulation 84, 1289–1295.

Waldo, K.L., Kumiski, D., Kirby, M.L., 1996. Cardiac neural crest is essential for the persistence rather than the formation of an arch artery. Dev. Dyn. 205, 281–292.

Waldo, K., Miyagawa-Tomita, S., Kumiski, D., Kirby, M.L., 1998. Cardiac neural crest cells provide new insight into septation of the cardiac outflow tract: aortic sac to ventricular septal closure. Dev. Biol. 196, 129–144.

Waldo, K.L., Zdanowicz, M., Burch, J., Kumiski, D.H., Godt, R.E., Creazzo, T.L., Kirby, M.L., 1999. A novel role for cardiac neural crest in heart development. J. Clin. Invest. 103, 1499–1507.

Waldo, K.L., Kumiski, D.H., Wallis, K.T., Stadt, H.A., Hutson, M.R., Platt, D.H., Kirby, M.L., 2001. Conotruncal myocardium arises from a secondary heart field. Development 128, 3179–3188.

Waldo, K.L., Hutson, M.R., Ward, C.C., Zdanowicz, M., Stadt, H.A., Kumiski, D., Abu-Issa, R., Kirby, M.L., 2005. Secondary heart field contributes myocardium and smooth muscle to the arterial pole of the developing heart. Dev. Biol. 281, 78–90.

Xu, H., Morishima, M., Wylie, J.N., Schwartz, R.J., Bruneau, B.G., Lindsay, E.A., Baldini, A., 2004. Tbx1 has a dual role in the morphogenesis of the cardiac outflow tract. Development 131 (13), 3217–3227.

Yelbuz, T.M., Waldo, K.L., Kumiski, D.H., Stadt, H.A., Wolfe, R.R., Leatherbury, L., Kirby, M.L., 2002. Shortened outflow tract leads to altered cardiac looping after neural crest ablation. Circulation 106, 504–510.

Yelbuz, T.M., Waldo, K.L., Zhang, X.W., Zdanowicz, M., Parker, J., Creazzo, T.L., Johnson, G.A., Kirby, M.L., 2003. Myocardial volume and organization are changed by failure of addition of secondary heart field myocardium to the cardiac outflow tract. Dev. Dyn. 228, 152–160.

Zaffran, S., Kelly, R.G., Meilhac, S.M., Buckingham, M.E., Brown, N.A., 2004. Right ventricular myocardium derives from the anterior heart field. Circ. Res. 95, 261–268.